Two-step Synthesis and Characterization of $MnCo_2O_4$ Composite and its Electrochemical Performance

ZhuChaozheng[1], Ma Yongzhi[2], Bu Qingkai[3], ZhouYanting[4], Wang Kai[4,*]

[1] College of Command and Control Engineering, Army Engineering University, Nanjing, 211117, China
[2] College of Mechanical and Electrical Engineering,Qingdao University,Qingdao, 266071,China
[3] School of Electronic and Information Engineering, Qingdao University,Qingdao, 266071,China
[4] College of Electrical Engineering, Qingdao University, Shandong Province, Qingdao, 266071, China
[*]E-mail: 15863060145@163.com

Supercapacitors are a novel kind of energy storage device. Two kinds of nanostructured materials of $MnCo_2O_4$ can be made using a two-step method. It can be proven that the nanosheet that grows evenly on the base of the nickel foam belongs to nanostructured $MnCo_2O_4$. Electrochemical experiments show that this $MnCo_2O_4$ composite has excellent electrochemical performance, which is similar to the novel structure of the mesoporous nanosheet of $MnCo_2O_4$. This $MnCo_2O_4$/composite material of nickel foam is a potential electrode material for supercapacitors. The structure and morphology of $MnCo_2O_4$ has an obvious influence on its electrochemical performance. The good structure and excellent performance suggest its promising application in supercapacitors.

1. INTRODUCTION

Supercapacitors can be called either electric double-layer capacitors or electrochemical capacitors [1-3]. They are a kind of energy storage element between a traditional static condenser and a storage battery [4-6]. They have many advantages, such as a shorter time for charging and discharging, a longer cycle life, as well as a larger specific power. These devices may be used in military applications, electric automobiles, wind power generation, solar power generation, and consumer electronics [7-9]. Previous studies of electrode materials mainly focus on carbon-based materials, metallic oxides, conducting polymers, etc.[10-12].

Among the electrode materials of supercapacitors that have been examined, metallic oxides have more advantages [13, 14]. Compared with carbon-based materials, metallic oxides have a higher

specific capacitance and energy density for its energy stores at the time of the redox reaction on the bulk phase and surface of the active material [15-18]. Compared with conducting polymers, metallic oxides have a relatively higher cycling stability and utilization ratio [19-21]. Furthermore, metallic oxides have more advantages, such as shape control, abundant storage, and so on [22-25]. Some ternary transition metal oxides, such as $NiCo_2O_4$, $CoFe_2O_4$ and $CoMn_2O_4$, will have a good effect on energy storage if they are used as the electrode material of a supercapacitor [26-31]. For example, the double-shelled $NiCo_2O_4$ hollow spheres exhibit ultrahigh specific capacitance and long cycle life when used in supercapacitor electrodes. Nanocage $MnCo_2O_4$ is synthesized by using a dual metal zeolitic imidazolate framework (ZIF, Mn-Co-ZIF) as both the precursor and the template, which shows great potential for a high-performance supercapacitor [32-35]. Cobalt-based metallic oxides with the ternary spinel structure are cobalt acid zinc, cobalt acid manganese, cobalt acid nickel, cobalt acid copper, cobalt acid magnesium, etc. [36-39].

A two-step method of hydrothermal synthesis and calcination is used in this article, making it possible to get composite electrode materials of cobalt acid manganese/nickel foam. As a result of the nanosheet superstructure, the material has a larger specific surface and abundant space, which is beneficial to the soak of the electrolyte and the transmission of the electronics. During cyclic voltammetry (CV) and galvanostatic charge-discharge testing, the composite electrode material of cobalt acid manganese/nickel foam shows excellent electrochemical performance. This cobalt acid manganese/nickel foam can be a potential supercapacitor electrode material.

2. EXPERIMENTAL

2.1. The method to make composite electrode materials of cobalt acid manganese /nickel foam

We used $Co(NO_3)_2 \cdot 6H_2O$ (2 mmol), $Mn(NO_3)_2 \cdot 4H_2O$ (1mmol), urea (6 mmol), and ammonium fluoride (12 mmol); another group without ammonium fluoride was used for comparison. All the raw materials were dissolved in 30 mL aqueous solution and stirred to mix well. The raw materials were placed in an ultrasound environment for 10 minutes. Then, the materials were poured into a reaction still. The nickel foam corroded by hydrogen chloride was rinsed with water and ethylalcohol and dried well. The nickel foam was then immersed aslant into the solution, and the reaction was still placed in a drying oven at 120 °C for 6 h. After the reaction, the nickel foam was rinsed with water and ethyl alcohol. To make the precursor of Mn-Co translate into $MnCo_2O_4$, the precursor of Mn-Co was placed in a drying oven at 70 °C and dried well. Then, it was placed into a muffle furnace to be calcined at 400 °C [25-28]. The rate of temperature rise was 5 °C/min. Then, it was held at 350 °C for approximately 2 h in a furnace and naturally cooled. The nickel foam with nanostructured $MnCo_2O_4$ had electrochemical performance testing directly as the electrode material of a supercapacitor.

2.2. The technology and method of materials characterization

The microstructure and the selection of EDS of composite electrode materials were analysed by scanning electron microscope (FE-SEM, JEOL, S-4800FE). The powder was scraped from the surface of the nickel foam and removed by magnet. The phase of the surface of the nickel foam material was

determined by a powder X-ray diffractometer (XRD utilizing a Cu Kα ray, wavelength of 0.154 nm, voltage of 40 kV, andcurrent of 40 mA). The 2-Theta range was between 10° and 70°.

2.3. Electrochemical performance testing of composite electrode materials of cobalt acid manganese /nickel foam

We used the three-electrode system CHI660D (ChenHua Instruments, Inc. ShangHai) to test the electrochemical performance. Saturated calomel worked as the reference electrode, which was compared to the foil electrode. CV (Cyclic Voltammogram) is a method by involving linear scanning voltage at a constantly accelerating velocity on the electrode. The moment it reaches the predetermined electric potential, it will scan reverse voltage and record the current electric potential curve. Finally, it shows the Cyclic Voltammogram curve. Galvanostatic charge-discharge (CD) is under constant current conditions, having both a charging and discharging operation for the electrode. We recorded the electric potential as a function of time.

3. RESULTS AND ANALYSIS

3.1 The analysis of XRD and EDX
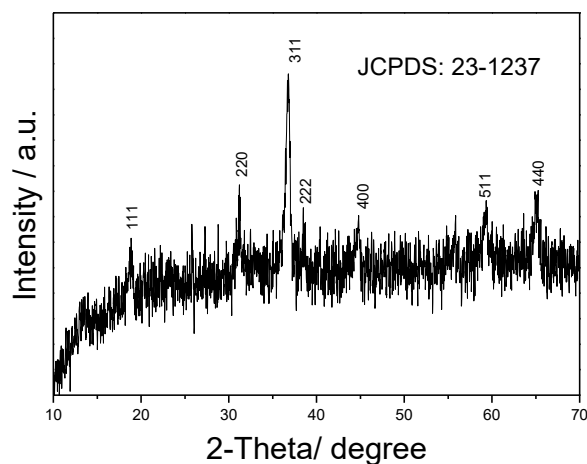
Figure 1. XRD diffraction pattern of the $MnCo_2O_4$ composite electrode materials

Fig. 1 is the XRD diffraction pattern of the $MnCo_2O_4$ composite electrode materials. The diffraction peak of the figure corresponds to the standard spectrogram of $MnCo_2O_4$ (JCPDS card file Number: 23-1237), indicating that the sample is phase pure. The sample with the less intense diffraction peak shows that the scale of the nanostructure is small, which can increase the number of effective electrochemical reaction points to improve the electrochemical performance.
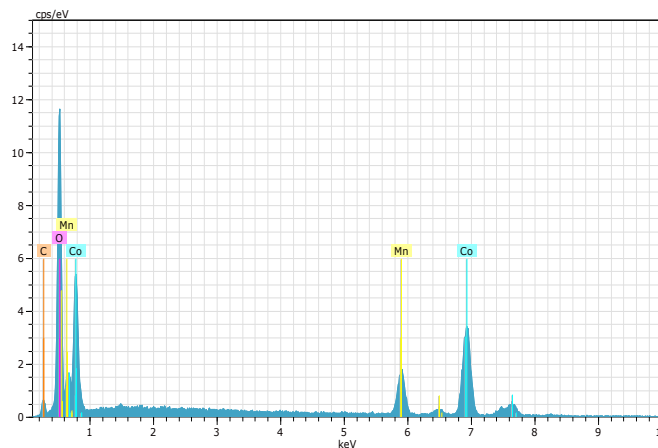
Figure 2. EDX energy spectrum diagram of $MnCo_2O_4$ composite electrode materials

Fig. 2 is the EDX energy spectrum diagram of $MnCo_2O_4$ composite electrode materials. The results show that Mn, Co and O are included in the nanostructure of the composite electrode materials of the cobalt acid manganese/nickel foam. Peak C in Fig. 2 is from the conductive adhesive of the SEM sample stage.

3.2 Analysis of SEM
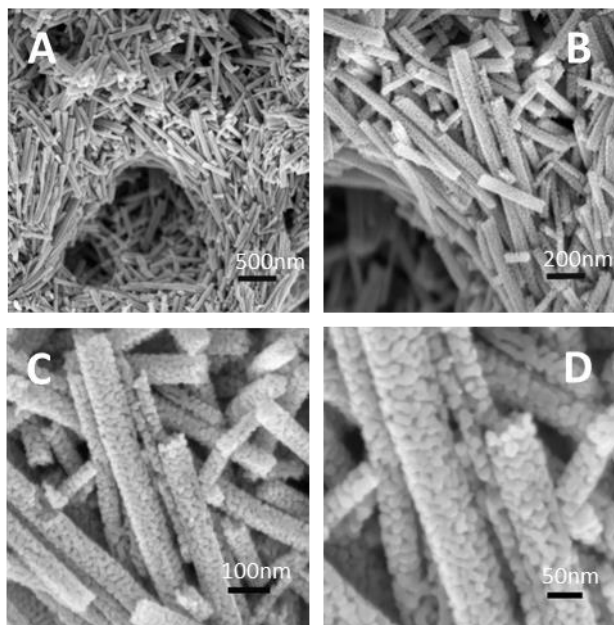
Figure3. SEM diagram of $MnCo_2O_4$ composite electrode materials without ammonium fluoride addition

Fig. 3 shows the SEM diagram of $MnCo_2O_4$ composite electrode materials without the addition of ammonium fluoride.). Fig. 3A and 3B show that the nanostructured $MnCo_2O_4$ evenly covers the surface of the nickel foam, and eventually forms the material of the electrode. Fig. 3C and 3Dare a high magnification of the SEM images, which show that the nanostructured $MnCo_2O_4$ which grows on the nickel foam is of the claviform structure with micron level. The diameter of the claviform structure

with micron level is 50 nm, and the length is between 200 nm and 500 nm. Fig. 3D shows that the scale of nanoparticle is almost 20 nm, which is very beneficial to the electrochemical performance.
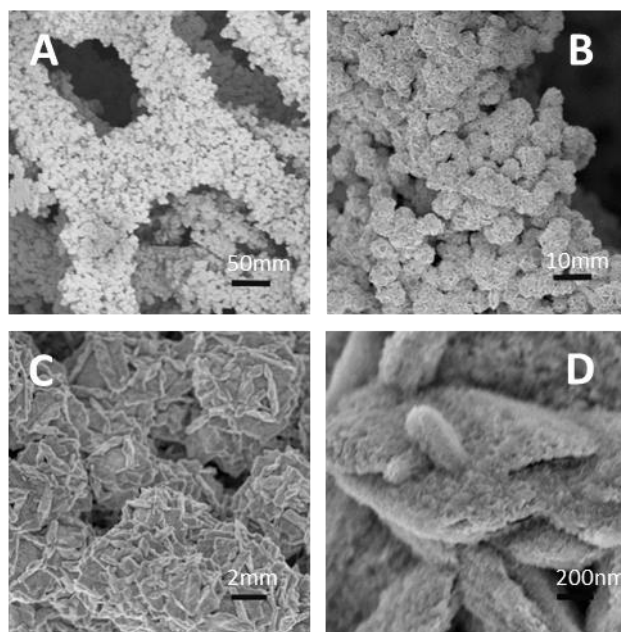
Figure 4. SEM diagram of $MnCo_2O_4$ composite electrode materials

Fig. 4 is an SEM diagram of $MnCo_2O_4$ composite electrode materials. Compared with Fig. 3, Fig. 4 adds ammonium fluoride during the preparation process. Figs. 4A and 4B show that the nanostructured $MnCo_2O_4$ evenly covers the surface of the nickel foam and eventually forms the material of the electrode. High magnification SEM images in Figs. 4C and 4D show that the nanostructured $MnCo_2O_4$, which grows on nickel foam, is of the laminated structure. The piece structure with micron level is composed of nanoparticles and there are many nanometre-sized gaps between pieces. Comparing Fig. 3 to Fig. 4 shows that the addition of ammonium fluoride during the material preparation process plays an important role in the morphology of the $MnCo_2O_4$.

3.3 Analysis of Cyclic Voltammogram

Fig. 5 is a Cyclic Voltammogram curve of composite electrode materials under varying scan rates. The rate ranges from 5 mV/s to 100 mV/s, and the voltage of the testing electrochemical window is from 0 to 0.5 V (vs. SCE). With an increase of the scan rate, the shape of the CV curves does not markedly change, showing that the active material utilization remains stable when electrochemical polarization and concentration polarization increase.
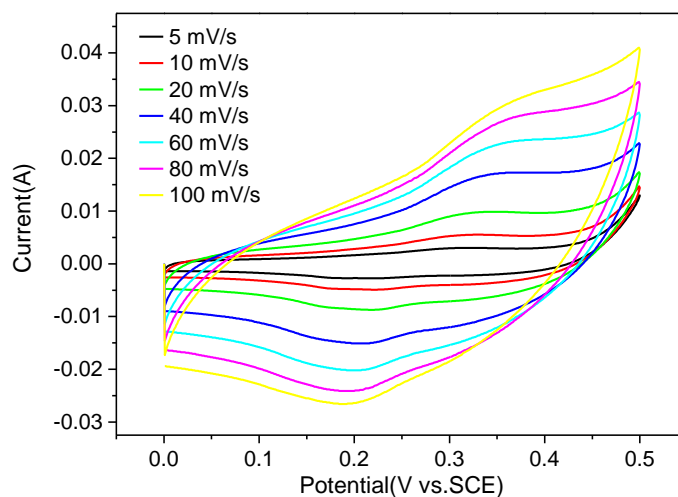
Figure 5. Cyclic Voltammogram curves of $MnCo_2O_4$ composite electrode materials without ammonium fluoride additionat at varying scan rates
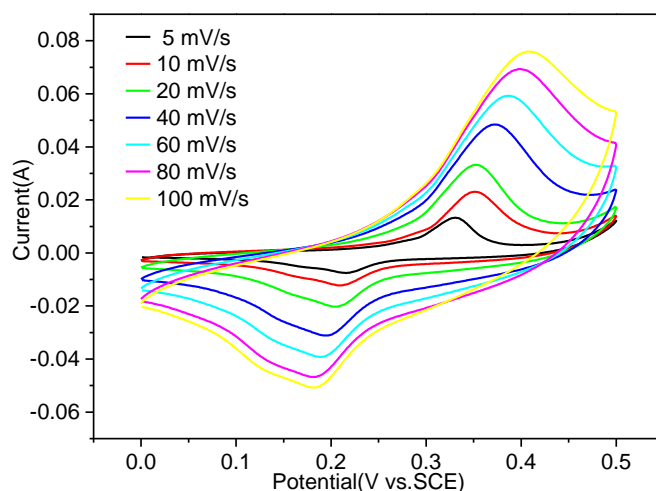
Figure 6. Cyclic Voltammogram curves of $MnCo_2O_4$ composite electrode materials at varying scan rates

Fig. 6 is a Cyclic Voltammogram curve of $MnCo_2O_4$ composite electrode materials at varying scan rates. The rate ranges from 5 mV/s to 100 mV/s, and the voltage of the testing electrochemical window is from 0 to 0.5 V (vs.SCE). There is a pair of obvious redox peaks in these CV curves. This finding indicates that the capacitance is mainly a pseudocapacitance behaviour of the materials, which is primarily due to the redox reaction. With the increase of scan rate, the shape of the CV curves does not markedly change, showing that it is more beneficial for the electrode materials to undergo a rapid redox reaction due to its unique micro-nanostructure. The pairs of redox current peaks correspond to the reversible reactions.

3.4 Analysis of Galvanostatic charge-discharge
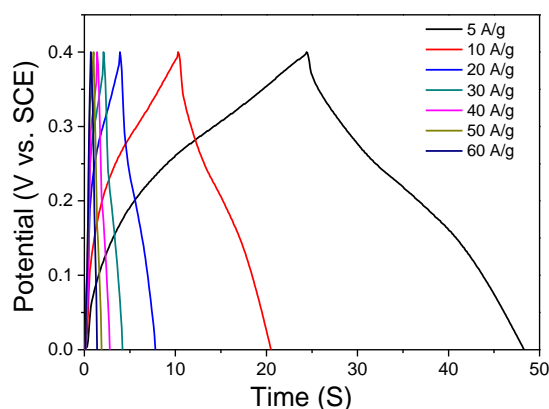
Figure 7. Galvanostatic charge-discharge curves of MnCo$_2$O$_4$ composite electrode materials without the addition of ammonium fluoride under varying ampere densities

Fig. 7 shows Galvanostatic charge-discharge curves of the composite electrode materials without the addition of ammonium fluoride under varying ampere densities. The density ranges from 5 A/g to 60 A/g, and the voltage of the testing electrochemical window ranges from 0 to 0.4 V (vs. SCE). The voltage doesn't reduce obviously on the discharge curve (compared with Fig. 8), showing that the inner resistance of the material is relatively small. The curve is nearly a triangle with symmetrical distribution, showing that the materials have good charging and discharging reversibility. There is an obvious linear relationship between voltage and time, showing that when it applies to a supercapacitor, there is slight pseudocapacitance behaviour (compared with Fig. 8). Using the equation C=Idt/md$V$ (where C is the specific capacitance (F/g), I is the current (A), m is the mass of active material (g), dt is the discharging time (s) and dV is the scanning voltage), the specific capacitance of the materials is 300 F/g when the ampere density is 5 A/g. The results suggest that these particles have a relatively higher capacitance than previously reported [18-20].
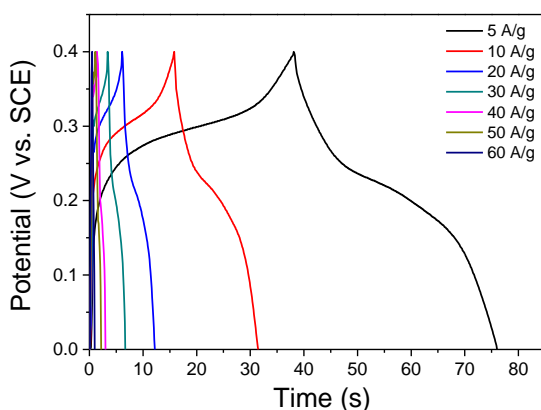
Figure 8. Galvanostatic charge-discharge curves of MnCo$_2$O$_4$ composite electrode materials under varying ampere densities

Fig. 8 shows Galvanostatic charge-discharge curves of MnCo$_2$O$_4$ composite electrode materials under varying ampere densities. The density ranges from 5 A/g to 60 A/g, and the voltage of the

testing electrochemical window ranges from 0 to 0.4 V (vs. SCE). The specific capacitance of the materials is 475 F/g when the ampere density is 5 A/g, which is higher than the materials of Fig. 7, showing that the micro-nanostructure of the materials has a big influence on its electrochemical performance. Compared with a previous report [16], it has a higher ampere density. This structure can not only provide more active reaction sites but also shorten the distance between the migrations of charge [18]. These results suggest that these particles have a relatively higher capacitance than previously reported [21-23].
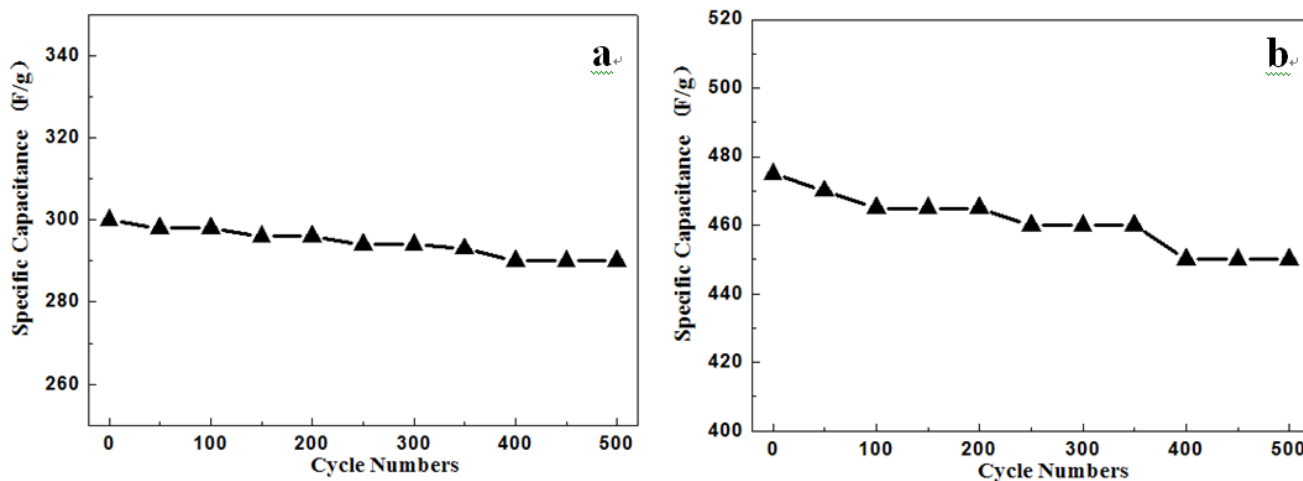
Figure 9. The charging/discharging cycle-life of cobalt acid manganese/nickel foam without the addition of ammonium fluoride (a) and cobalt acid manganese/nickel foam (b) at a current density of 5 A•g^{-1} for 500 cycles

Under the current density of 5A·g^{-1}, the charging/discharging cycle-life of cobalt acid manganese/nickel foam with and without the addition of ammonium fluoride was tested500 times, and the specific capacity as a function of the cycle number is shown in Fig. 9. The initial capacity of the cobalt acid manganese/nickel foam without the addition of ammonium fluoride was 300 F·g^{-1}.The specific capacity was 290 F·g^{-1} after 500cycles, yielding a capacity retention rate of 96.7%. The initial capacity of the cobalt acid manganese/nickel foam with ammonium fluoride addition was 475 F·g^{-1} and the specific capacity was 450 F·g^{-1} after 500 cycles, yielding a capacity retention rate of 94.7%. These results are better than the results reported in a previous study [20].

4. CONCLUSIONS AND DISCUSSION

Nanostructured $MnCo_2O_4$ materials can grow directly on the base of nickel foam by a two-step method, and electrochemical performance testing shows that these materials can be used as electrode materials of a supercapacitor. During preparation, ammonium fluoride plays an important role on the morphology. It was shown that the nanosheet that grows evenly on the base of the nickel foam belongs to nanostructured $MnCo_2O_4$. The electrochemical property testing shows that this composite electrode has excellent electrochemical performance which is closely connected to the novel structure of the

mesoporous nanosheet of $MnCo_2O_4$. This impressive performance of the $MnCo_2O_4$/composite material of nickel foam was found to be better than that of many literature reports on the compound materials. Specific capacitance was observed to be as high as 475 F/g when the ampere density is 5 A/g. $MnCo_2O_4$/composite material is a potential electrode material for supercapacitors. The structure and morphology of nanostructured $MnCo_2O_4$ have a substantial influence on its electrochemical performance. The good structure and excellent performance of these materials indicate their promising application in supercapacitors.

References

1. H. Hu, B.Y. Guan and X.W. Lou, *Chem.*, 1 (2016) 102.
2. Y.P. Fu, J.L. Ding, H.F. Wang and J.W. Wang, *Appl. Soft Comput.*, 68 (2018) 847.
3. K. Wang and L. Zhang, *Int. J. Electrochem. Sci.*, 8 (2013) 2892.
4. K. Wang and L. Zhang, *Electrochemistry*, 81 (2013) 259.
5. N.Li, S.F. Tang, Y.D. Rao, J.B. Qi, P.K. Wang, Y. Jiang, H.M. Huang, J.M. Gu and D.L. Yuan, *Electrochim. Acta*, 270 (2018) 330.
6. H. Hu, Z.B. Zhao, Q. Zhou, Y. Gogotsi and J.S. Qiu, *Carbon*, 50 (2012) 3267.
7. K. Wang, L.W. Li, T.Z. Zhang and Z.F. Liu, *Energy*, 2014, 70 (2014) 612.
8. W.Z. Qu and W. Chen. *Adv. Appl. Math. Mech.*, 7 (2015) 13.
9. K. Wang, L.W. Li and T.Z. Zhang, *Int. J. Electrochem. Sci.*, 8 (2013) 6900.
10. K. Wang, L.W. Li, H.X. Yin and W.B. Wan, *Plos One*, 10 (2015) e0138672.
11. H. Hu, J.T. Zhang, B.Y. Guan and X.W. Lou, *Angew Chem. Int. Ed.*, 33 (2016) 9666.
12. F.J. Wang, C.S. Liu and W.Z. Qu, *Appl. Math. Lett.*, (2018), https://doi.org/10.1016/j.aml.2018.07.002.
13. K. Wang, L. Zhang, B.C. Ji, J.L. Yuan, *Energy*, 59 (2013) 440.
14. H. Hu, L. Han, M. Yu, Z. Wang and X.W. Lou, *Energy Environ. Sci.*, 9 (2017) 107.
15. K. Wang, L.W. Li and T.Z. Zhang, *Int. J. Electrochem. Sci.*, 8 (2013) 6252.
16. F.J. Wang, Q.S. Hua and C.S. Liu, *Appl. Math. Lett.*, 84 (2018) 130.
17. K. Wang, L. Zhang, Y.H. Jin and Y. Fan, *Russ. J. Electrochem.*, 50 (2014) 176.
18. T. Pichler, *Nature Mater.*, 6 (2007) 332.
19. Y. Gu, X.Q. He, W. Chen and C.Z. Zhang, *Comput. Math. Appl.*, 75 (2018) 33.
20. H. Hu, L. Han, M. Yu, Z. Wang and X.W. Lou, *Energy Environ. Sci.*, 9 (2016) 107.
21. J. Bhagwan, V. Sivasankaran, K.L. Yadav and Y. Sharma, *J. Power Sources*, 327 (2016) 29.
22. K. Wang, L.W. Li and X.Z. Wu, *Int. J. Electrochem. Sci.*, 8 (2013) 6574.
23. K. Wang, L.W. Li and X.Z. Wu, *Int. J. Electrochem. Sci.*, 8 (2013) 6763.
24. D.K. Mishra, H.J. Lee and J. Kim, *Green Chem.*, 19 (2017) 1619.
25. C.H. Zhang, Y.G. Kao, B.H. Kao and T.Z. Zhang, *Appl. Math. Comput.*, 337 (2018) 399.
26. H.T. Wu, S. Wang, Y. Wang, F. Wang and David W, *ACS Appl. Mater. Interfaces*, 10 (2017) 1021.
27. S.F. Tang, D. Yuan, Y. Rao, N. Li, J. Qi, T. Cheng, Z. Sun, J. Gu and H. Huang, *Chem. Eng. J.*, 337 (2018) 446.
28. H. Hu, Z.B. Zhao, W. Wan, Y. Gogotsi and J.S. Qiu, *Adv. Mater.*, 25 (2013) 2219.
29. Y. Ren, C.G. Sun, M.J. Song and L.T. Wang, *Int. J. Electrochem. Sci.*, 11 (2016) 10706.

30. L. Zhang, H.D. Liu, H.B. Ruan and Y.Y. Su, *Int. J. Electrochem. Sci.*, 11 (2016) 10815.
31. L.Q. Lu, S.M. Xu and J.W. An, *Int. J. Electrochem. Sci.*, 11 (2016) 9687.
32. K. Wang, J.B. Pang, L.L. Li, S.Z. Zhou, Y.H. Li and T.Z. Zhang, *Front. Chem. Sci. Eng.*, (2018), https://doi.org/10.1007/s11705-018-1705-z.
33. K. Wang, L.W. Li, W. Xue, S.Z. Zhou, Y. Lan, H.W. Zhou and Z.Q. Sui, *Int. J. Electrochem. Sci.*, 12 (2017) 8306.
34. Y.P. Fu, H.F. Wang, G.D. Tian, Z.W. Li and H.S. Hu, *J. Intell. Manuf.*, (2018). https://doi.org/10.1007/s10845-017-1385-4.
35. Y.P. Fu, G.D. Tian, Z.W. Li and Z.L. Wang, *IEEJ Trans. Electr. Electron. Eng.*, 13 (2018) 748.
36. W.Z. Qu, W. Chen and Y. Gu, *Comput. Math. Appl.*, 70 (2015) 679.
37. K. Wang, C. Li, B. Ji, *J. Mater. Eng. Perform.*, 23 (2014) 588.
38. K. Wang, L.W. Li and H.W. Zhang, *Int. J. Electrochem. Sci.*, 8 (2013) 5036.
39. K. Wang, S.Z. Zhou, Y.T. Zhou, J. Ren, L.W. Li and Y. Lan, *Int. J. Electrochem. Sci.*, 13 (2018), https://doi.org/10.20964/2018.11.30.